Tri-Polar Concentric Ring Electrode Development for Laplacian Electroencephalography

Walter G. Besio, *Senior Member, IEEE*, Kanthaiah Koka*, Rajesh Aakula, and Weizhong Dai

***Abstract*—Brain activity generates electrical potentials that are spatio-temporal in nature. Electroencephalography (EEG) is the least costly and most widely used noninvasive technique for diagnosing many brain problems. It has high temporal resolution, but lacks high spatial resolution. In an attempt to increase the spatial selectivity, researchers introduced a bipolar electrode configuration utilizing a five-point finite difference method (FPM) and others applied a quasi-bipolar (tri-polar with two elements shorted) concentric electrode configuration. To further increase the spatial resolution, the authors report on a tri-polar concentric electrode configuration for approximating the analytical Laplacian based on a nine-point finite difference method (NPM). For direct comparison, the FPM, quasi-bipolar method (a hybrid NPM), and NPM were calculated over a 400 $\times$ 400 mesh with 1/400 spacing using a computer model. A closed-form analytical computer model was also developed to evaluate and compare the properties of concentric bipolar, quasi-bipolar, and tri-polar electrode configurations, and the results were verified with tank experiments. The tri-polar configuration and the NPM were found to have significantly improved accuracy in Laplacian estimation and localization. Movement-related potential (MRP) signals were recorded from the left prefrontal lobes on the scalp of human subjects while they performed fast repetitive movements. Disc, bipolar, quasi-bipolar, and tri-polar electrodes were used. MRP signals were plotted for all four electrode configurations. The signal-to-noise ratio and spatial selectivity of the MRP signals acquired with the tri-polar electrode configuration were significantly better than the other configurations.**

***Index Terms*—Bipolar, EEG, five-point method, MRP, nine-point method, spatial selectivity, surface Laplacian, tri-polar.**

I. Introduction

H. BERGER recorded the first human electroencephalography (EEG) from the scalp in 1924. Currently, EEG still is the most important noninvasive method for investigation of neural activity of the brain [1]. Among the different methods utilized for recording brain activity, EEG is the cheapest and produces sufficient temporal resolution to enhance the study of complex brain functions. An EEG system requires only a few milliseconds for acquiring scalp surface electrical activity, which is much faster than functional magnetic resonance imaging and positron emission tomography.

A significant drawback of EEG, however, is that it lacks high spatial resolution, primarily due to the blurring affects of the volume conductor with disc electrodes. Conventional EEG signals recorded with disc electrodes have reference electrode problems as idealized references are not available with EEG [2]. Much advancement has come in recent years to improve EEGs appeal for brain activity analysis. One such advancement is the application of surface Laplacian to EEG. Surface Laplacian mapping has been shown to enhance the high spatial frequency components and spatial selectivity of the electrical activity located close to the observation point [3]. These unique characteristics are based on the surface Laplacian being the second spatial derivative of the surface potentials.

The application of the Laplacian method to study EEG commenced with Hjorth [4] utilizing a five-point method (FPM). He [3] calculated the surface Laplacian with Hjorth's technique derived from an array of disc electrodes measuring surface potentials. Several other approaches have revealed positive results as well in the estimation of the scalp Laplacian resulting from the EEG potential measurements. Unique approaches include the spline Laplacian algorithm reported by Perrin *et al.* [5] and the ellipsoidal spline Laplacian algorithm disclosed by Law *et al.* [6], in addition to realistic Laplacian estimation techniques by Babiloni *et al.* [7], [8] and realistic geometry Laplacian algorithms [9].

Fattorusso and Tilmant [10] were the first investigators to report the use of concentric ring electrodes. He and Cohen [11] proposed bipolar concentric ring Laplacian electrodes for measuring the Laplacian potential directly from the body surface and an array of these electrodes were used to create body surface Laplacian maps for cardiac signals. The concentric ring electrodes can resolve the reference electrode problems as discussed by Nunez [2] since concentric ring electrodes act like closely spaced bipolar recordings. Concentric ring electrodes are symmetrical alleviating electrode orientation problems [12]. They also act as spatial filters reducing the low spatial frequencies and increasing the spatial selectivity [12].

To further improve the spatial resolution of EEG, this paper discusses a novel Laplacian EEG (LEEG) tri-polar concentric ring electrode configuration [Fig. 1(C)]. These tri-polar concentric ring electrodes can measure the Laplacian potential directly [13], [14]. Such a configuration was compared against bipolar [Fig. 1(A)], and quasi-bipolar [Fig. 1(B)] electrode configurations [15] for accuracy in approximating the analytical Laplacian, spatial resolution, and localization. This tri-polar

Manuscript received June 15, 2005; revised October 15, 2005. This work was supported in part by the Louisiana Tech University CEnIT and in part by Louisiana Board of Regents under Grant LEQSF(2003-05)-RD-B-05. *Asterisk indicates corresponding author.*

W. G. Besio is with the Biomedical Engineering Department, Louisiana Tech University, Ruston, LA 71270 USA (e-mail: walterb@latech.edu).

*K. Koka is with the Biomedical Engineering Department, Louisiana Tech University, Ruston, LA 71270, USA (e-mail: kanthu@gmail.com).

R. Aakula was with the Electrical Engineering Department, Louisiana Tech University, Ruston, LA 71270 USA.

W. Dai is with Department of Mathematics and Statistics, Louisiana Tech University, Ruston, LA 71270 USA.

Digital Object Identifier 10.1109/TBME.2005.863887

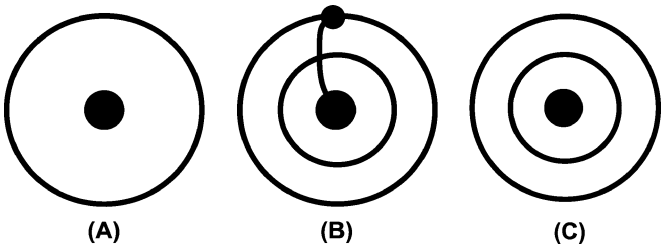

Fig. 1. Configurations for (A) bipolar electrode, (B) quasi-bipolar electrode, and (C) tri-polar electrode. The quasi-bipolar electrode configuration is obtained by shorting the inner disc to the outer ring as shown by the arc in (B).

configuration is based upon a numerical approximation technique, the nine-point method (NPM), which is commonly used in image processing for edge detection. Computer modeling of the concentric ring electrodes and the verification with data collected from tank experiments are also reported. Finally, movement-related potential (MRP) signals [16] recorded from human subjects using gold disc electrodes and concentric ring bipolar, quasi-bipolar and tri-polar electrodes are presented.

II. Theoretical Background

A. Five-Point Method

As shown in Fig. 2, v_0 through v_8 are the potentials at points p_0 through p_8, respectively. To simplify the narrative, v_0 through v_8 may also signify points p_0 through p_8. v_5, v_6, v_7, v_8, and v_0, with a spacing of $2r$ are applied in the FPM (a bipolar electrode configuration approximation), as in (1). This follows Huiskamp's [17] calculation of the Laplacian with the exception of the use of $2r$. The $2r$ is necessary for a direct comparison of the three electrode configurations analyzed. The Laplacian potentials at point p_0 are calculated as

$$\Delta v_0 = \frac{\partial^2 v}{\partial x^2} + \frac{\partial^2 v}{\partial y^2} = \frac{1}{(2r)^2}\left(\sum_{i=5}^{8} v_i - 4v_0\right) + O\left((2r)^2\right) \quad (1)$$

where

$$O\left((2r)^2\right) = \frac{(2r)^2}{4!}\left(\frac{\partial^4 v}{\partial x^4} + \frac{\partial^4 v}{\partial y^4}\right) + \frac{(2r)^4}{6!}\left(\frac{\partial^6 v}{\partial x^6} + \frac{\partial^6 v}{\partial y^6}\right) + \cdots$$

is truncation error and can be neglected according to Lapidus and Pinder [18]. Therefore, the approximation to the Laplacian at p_0 is

$$\Delta v_0 \cong \frac{4}{(2r)^2}(\overline{v} - v_0) \quad (2)$$

where $\overline{v}$ is the average of the potentials v_5, v_6, v_7, and v_8 corresponding to points $\mathrm{p}_5 \sim \mathrm{p}_8$.

Equation (2) can be applied to a bipolar configuration (a concentric ring and disc) by taking the integral along a circle of radius $2r$ from point p_0 and defining $\mathrm{X} = 2\mathrm{r}\cos(\theta)$ and $\mathrm{Y} = 2\mathrm{r}\sin(\theta)$ as in Huiskamp [17]. This leads to (3)

$$\Delta v_0 \cong \frac{4}{(2r)^2}\left[\frac{1}{2\pi}\int_0^{2\pi} v(2r,\theta)d\theta - v_0\right]. \quad (3)$$

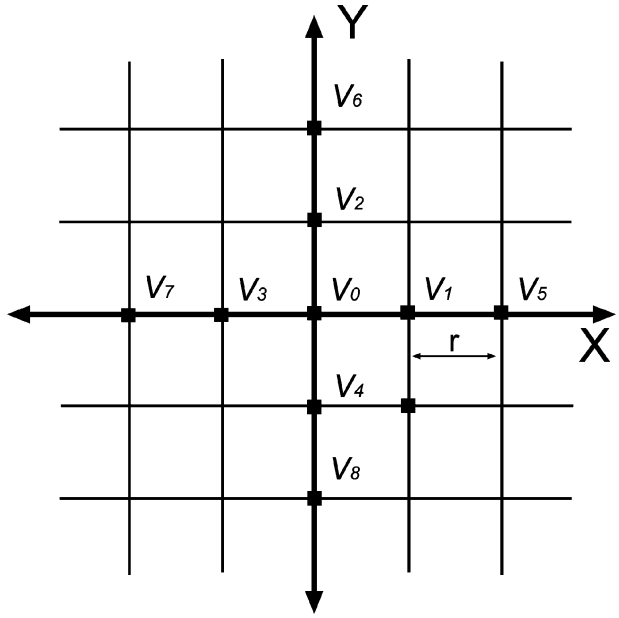

Fig. 2. Arrangement of the FPM, quasi-bipolar method and NPM on a regular plane square grid of size $\mathrm{N} \times \mathrm{N}$ and spacing $\mathrm{h} = 1/\mathrm{N}$ with interpoint distance $\mathrm{r} = \mathrm{nh}$, where $\mathrm{n} = 1, 2, 3 \ldots$ v_0 through v_8 are the potentials at points p_0 through p_8, respectively. v_5, v_6, v_7, v_8, and v_0 form the FPM, v_1, v_2, v_3, v_4, v_5, v_6, v_7, v_8, and v_0 form the quasi-bipolar method and NPM, except that v_5, v_6, v_7, and v_8 are shorted to v_0 for the quasi-bipolar method.

Solving the integration in (3) leaves

$$\Delta v_0 \cong \frac{4}{(2r)^2}(\overline{v} - v_0) \quad (4)$$

where $\overline{v} = (1/2\pi)\int_0^{2\pi} v(2r,\theta)d\theta$ is the average potential on the concentric outer ring.

B. Quasi-Bipolar Method

In the quasi-bipolar method [15], the outer ring and center disc are shorted together as shown in Fig. 1(B). The Laplacian potential is calculated as (5)

$$\Delta v_0 = \frac{(\overline{v} + v_0)}{2} - v_m. \quad (5)$$

Here, $\overline{v}$ is the average potential on the outer ring, v_m is the average potential on the middle ring and v_0 is the average potential on the center disc.

C. Nine-Point Method

The NPM can be viewed as two FPMs: as shown in Fig. 2, points v_1, v_2, v_3, v_4, and v_0 form one FPM with a spacing of r; points v_5, v_6, v_7, v_8, and v_0 form a second FPM with a spacing of $2r$. The Laplacian potentials at point p_0 due to these potentials are given in (6)

$$\Delta v_0 = \left(\frac{\partial^2 v}{\partial x^2} + \frac{\partial^2 v}{\partial y^2}\right) = \frac{1}{12r^2}\left\{16\sum_{i=1}^{4} v_i - 60v_0 - \sum_{j=5}^{8} v_j\right\} + 0(r^4) \quad (6)$$

where $O(r^4) = (r^4/270)((\partial^6 v/\partial x^6) + (\partial^6 v/\partial y^6)) + \cdots$ is the truncation error.

Comparison of (1) and (6) reveals that the NPM truncation error does not have the fourth-order derivative term. Therefore, the NPM is more accurate than the FPM.

By applying a similar procedure as was used for the bipolar configuration, taking the integral along a circle of radius r around point p_0 and defining $\mathrm{X} = \mathrm{r}\sin(\theta)$, $\mathrm{Y} = \mathrm{r}\cos(\theta)$ as in Huiskamp [17] results in the following for the middle ring and disc:

$$\frac{1}{2\pi}\int_0^{2\pi} v(r,\theta)d\theta - v_0 = \frac{r^2}{4}2\pi\Delta v_0 + \frac{r^4}{4!}\int_0^{2\pi}\sum_{j=0}^{4}(\sin\theta)^{4-j}(\cos\theta)^j d\theta\left(\frac{\partial^4 v}{\partial x^{4-j}\partial y^j}\right) + \cdots. \quad (7)$$

Similarly, by applying the integral along a circle of radius $2r$ around point p_0, the following is obtained for the outer ring and disc:

$$\frac{1}{2\pi}\int_0^{2\pi} v(2r,\theta)d\theta - v_0 = r^2 2\pi\Delta v_0 + \frac{2r^4}{3}\int_0^{2\pi}\sum_{j=0}^{4}(\sin\theta)^{4-j}(\cos\theta)^j d\theta\left(\frac{\partial^4 v}{\partial x^{4-j}\partial y^j}\right) + \frac{(2r)^6}{6!}\int_0^{2\pi}\sum_{j=0}^{6}(\sin\theta)^{6-j}(\cos\theta)^j d\theta\left(\frac{\partial^6 v}{\partial x^{6-j}\partial y^j}\right) + \cdots. \quad (8)$$

Multiplying (7) by 16 and subtracting (8) cancels the fourth-order term, resulting in the Laplacian approximation

$$\Delta v_0 \cong \frac{1}{3r^2}\left\{16\left(\frac{1}{2\pi}\int_0^{2\pi} v(r,\theta)d\theta - v_0\right) - \left(\frac{1}{2\pi}\int_0^{2\pi} v(2r,\theta)d\theta - v_0\right)\right\} \quad (9)$$

where $(1/2\pi)\int_0^{2\pi} v(r,\theta)d\theta$ represents the potential on the middle ring of a tri-polar configuration, and $(1/2\pi)\int_0^{2\pi} v(2r,\theta)d\theta$ represents the potential on the outer ring. Therefore, the NPM can be translated into a tri-polar concentric electrode configuration.

III. Methodology

A. Comparison of Laplacian Approximations of FPM, Quasi-Bipolar Method and NPM Using Finite Computer Model

Finite difference methods have been used to approximate the Laplacian [3], [4] in the past; therefore, a comparison of the accuracy for the popular finite difference methods was performed. A mesh of 400×400 was modeled with a spacing of 1/400. On each point of this mesh, the FPM, quasi-bipolar method, and NPM were applied for approximating the Laplacian with appropriate boundary conditions. This process was repeated for interelectrode distances from $\mathrm{r} = 1$ to 20. These estimates were then compared with the calculated analytical Laplacian for each point of the mesh. To calculate the analytical Laplacian, the electric potential Φ generated by a dipole in a homogeneous medium of conductivity σ was calculated using the formula for the electrical potential, as in He and Wu [19]

$$\phi = \frac{1}{4\pi\sigma}\cdot\frac{(\overline{r_p} - \bar{r})\bullet\overline{P}}{|\overline{r_p} - \bar{r}|^3}. \quad (10)$$

The second derivative of the potential was performed [19], $L = \Delta\phi = (\partial^2\phi/\partial x^2) + (\partial^2\phi/\partial y^2)$, resulting in (11)

$$L = \frac{3}{4\pi\sigma}\left[5(z_p - z)^2\frac{(\overline{r_p} - \bar{r})\bullet\bar{P}}{|\overline{r_p} - \bar{r}|^7} - \frac{(\overline{r_p} - \bar{r})\bullet\bar{P} + 2(z_p - z)p_z}{|\overline{r_p} - \bar{r}|^5}\right]. \quad (11)$$

The Laplacian potentials of the FPM, quasi-bipolar method and NPM were compared with the analytical solution by calculating the relative error and maximum error [17]

$$\text{Relative Error } i = \left[\frac{\sum(\Delta v - \Delta^i v)^2}{\sum(\Delta v)^2}\right]^{\frac{1}{2}} \quad (12)$$

$$\text{Maximum Error } i = \max|\Delta v - \Delta^i v| \quad (13)$$

where i represents the method (FPM, quasi-bipolar method, or NPM) used to approximate the Laplacian and Δv represents the analytical Laplacian potential. The comparisons are shown figuratively in Section IV for the different interelectrode distances analyzed.

B. Closed-Form Moving Dipole Analytical Computer Model

To more realistically approximate concentric ring electrode configurations than the finite difference methods, based on (10), a closed-form analytical computer model, illustrated in Fig. 3, was designed to calculate the potential due to a moving dipole in a medium of constant conductivity σ. In this computer model, $[1/(4\pi\sigma)]$ was taken as a constant, pertaining to the conductivity

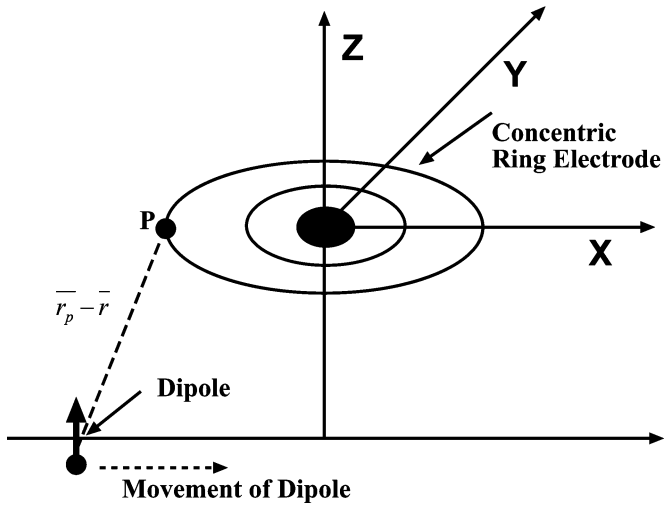

Fig. 3. Concentric ring electrode configuration for the closed-form moving dipole computer model. The dipole directed toward the positive Z-axis was moved incrementally 1.0 cm at a time from the depth of -1.0 to -4.0 cm. The dipole was also moved horizontally from -5.0 to 5.0 cm along the X-axis.

of saltwater and the permittivity of the material used for the dipole preparation. These model properties will be discussed further in Section IV.

For the moving dipole model, the outer concentric ring ranged from 5 to 36 mm in diameter with the disc and middle ring sized proportionally from 0.4 to 5 mm and 2.5 to 10 mm, respectively. An axial dipole, directed toward the positive Z-axis, was moved incrementally 0.5 cm at a time along the Z-axis from depths of -0.5 to -2.0 cm. The dipole traversed the X-axis from -5.0 to 5.0 cm and along $\mathrm{Y} = 0\ \mathrm{cm}$ line. First, the depth of the dipole was kept constant while the dipole was moved along the X-axis. Then, the depth of the dipole was changed and moved along the X-axis again. From the simulated model of the moving dipole, the potentials on each electrode element were calculated using (10). These potentials were then used to calculate the Laplacian of the bipolar electrode with (4), quasi-bipolar electrode using (5) as reported in [15], and the tri-polar electrode with (9). From the calculated Laplacian potentials for the bipolar, quasi-bipolar, and tri-polar electrode configurations, the attenuation in decibels of the calculated potentials along the radial direction was also calculated and plotted.

The above computer simulations were repeated using a constant unit dipole at a depth of 1 cm below the origin and 20 unit dipoles at random locations limited to a space of 12 cm $\times$ 12 cm centered at the origin. The constant unit dipole was always active and three or four random dipoles were kept active during the simulation. The potentials on the elements of the electrodes were calculated using (10). The Laplacian potentials were calculated for different electrode systems, namely bipolar with (4), quasi-bipolar with (5) and tri-polar with (9), and localization [20] characteristics were determined for the three electrode configurations and plotted.

C. Tank Experiments

Tank experiments were conducted in order to verify the results obtained by the closed-form moving dipole computer model. A plexi-glass tank of size $50\ \mathrm{cm} \times 26\ \mathrm{cm} \times 30\ \mathrm{cm}$ was filled with a saltwater mixture of 9 gm/L concentration, similar to that of human intracellular space. A dipole was constructed with two thin 1 mm radius copper discs, which were identically etched on both sides of a printed circuit board. Two 5–V peak-to-peak, 100-Hz ac square waves were then applied between the discs. The two discs were given alternating polarity square waves in order to limit the corrosion of the dipole discs.

The concentric electrodes were designed with ORCAD (Cadence) software and prepared using an LPKF ProtoMat C20 rapid prototype board plotter (LPKF Laser & Electronics). The concentric electrodes were attached to a lead screw driven stage (T2312-A.5, Bell Screws & Actuators Co.) and moved along the X-axis on the surface of the saltwater at the rate of 1.8 cm/s. The experiment was repeated 20 times with a constant dipole depth and the data were averaged to minimize variations due to the experimental setup. Then the depth was changed and the measurements were repeated until all five depths, 0.5, 1.0, 1.5, 2.0, and 2.5 cm, were completed.

For comparison, the electrode elements in the tank experiments matched one set of electrode parameters in the closed-form moving dipole computer model. The outer ring was set at 10 mm radius. The middle rings for the quasi-bipolar and tri-polar configurations were set at 5-mm radius. The disc had a radius of 0.4 mm. The widths of the outer and middle rings were both set at 0.4 mm. The depth of the dipole was set at 1.0 cm below the surface of the electrode. In the tank experiments, the electrode was moved in the direction of the X-axis on the surface of the saltwater solution while the dipole was set stationary at the location of $\mathrm{X} = \mathrm{Y} = 0.0\ \mathrm{cm}$.

Potential measurements were taken from the three elements of the concentric ring electrodes using a custom LabView (National Instruments) program via a National Instruments DaqCard 700. An exposed electrode between the dipole discs referenced the measurements. Post processing was achieved with a custom Matlab (Mathworks) program. Laplacian potentials were calculated for bipolar, quasi-bipolar, and tri-polar electrode configurations using (4), (5), and (9), respectively. The attenuation of the signal due to the distance along the radial axis was calculated and attenuation in decibels was plotted for comparison between the three electrode configurations. The attenuation values are a measure of the localization [21] and global noise rejection abilities of the three electrode configurations.

D. Movement-Related Potential (MRP) Recording

All the recordings were conducted in accordance with the IRB protocols. The MRP signals were recorded using a 1-cm gold disc electrode (Grass F-E5GH) and concentric ring electrodes from ten volunteers (ages from 23 to 27 years, 4 females and 6 males, all were right handed) who gave informed consents. The subjects were seated in a comfortable chair with their right hand kept on the table in front of them. The subjects were asked to keep their right index finger on a micro-switch and close their eyes to minimize the eye movement artifacts. The subjects were asked to press the micro-switch once per second cued by a metronome. Signals from EEG and the micro-switch were recorded for 5 min.

The recordings were performed twice on each subject, once with a gold disc electrode and again with a tri-polar concentric ring electrode ($\mathrm{outer\ ring\ diameter} = 2.0\ \mathrm{cm}$ and $\mathrm{middle\ ring\ diameter} = 1.4\ \mathrm{cm}$). The electrodes were kept on the left prefrontal lobes (FP1) according to 10/20 international system. A preamplifier was built with a gain of 20 and a high-pass cutoff of 0.1 Hz. The preamplifier was followed by a Grass 15LT amplifier with the passband set from 0.3 Hz to 30 Hz and gain of 2000 (total gain of 40 000) for concentric ring electrodes and 500 (total gain of 10 000) for gold disc electrodes. A National Instruments DaqCard 6036E was used to acquire the signals with a custom LabView program at 250 s/s. The skin-to-electrode impedance was kept below 10 kOhms.

The acquired data were then processed with a custom Matlab program. The micro-switch signal was recorded as a time reference. The EEG and LEEG were divided into windows of 1 s (499 ms before and 501 ms after the movement). The trials contaminated with eye and head movements were removed. Approximately 150–200 artifact free windows remained and were averaged. The LEEG was calculated for each concentric ring electrode for bipolar, quasi-bipolar, and tri-polar electrode configurations using the respective formulae and plotted. The

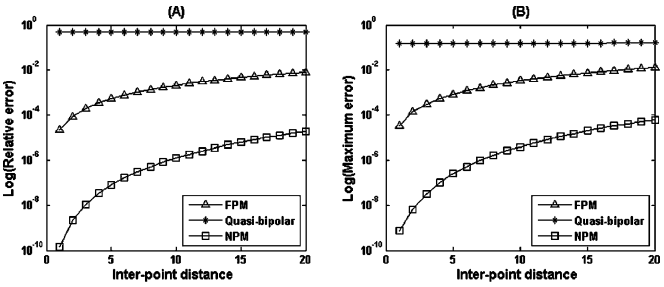

Fig. 4. (A) Relative error and (B) maximum error of FPM, quasi-bipolar method, and NPM, respectively, when compared to the analytical value of the Laplacian.

source separation [12] using each electrode system was calculated and compared as the ratio of the peak signal divided by the length of the window. The peak signal-to-noise ratio (SNR) [21] was calculated using (14) for each electrode configuration. The peak signal was taken as the length of the signal up to the second zero-crossing prior to the positive peak and one zero-crossing after the positive peak; the remainder of the window was taken as the noise signal

$$\mathrm{SNR} = \frac{E_{\mathrm{peak}}}{E_{\mathrm{noise}}} = \frac{\frac{1}{P}\sum_{i=1}^{p} x_i^2}{\frac{1}{n}\sum_{j=1}^{n} x_j^2}. \tag{14}$$

For (14), E is the energy, x_i is amplitude of the signal, p is the number of points in the peak, and n is the number points in the noise.

IV. Results

A. Error Comparison Between FPM, Quasi-Bipolar Method and NPM Using the Finite Difference Model

Relative and maximum errors of the FPM, quasi-bipolar method, and the NPM were calculated using (12) and (13). The results were plotted for different interpoint distances, as shown in Fig. 4(A) for relative error and Fig. 4(B) for maximum error. A Bonferroni t test showed that there are statistically significant differences in the relative errors and maximum errors of the FPM, quasi-bipolar method, and the NPM at the 1% significance level, respectively. The NPM has the least relative error and maximum error among the three electrode configurations analyzed.

B. Calculation of Laplacian Potential and Localization Effect for the Three Different Concentric Ring Electrode Configurations

Laplacian potentials measured from the tank experiments for bipolar, quasi-bipolar, and tri-polar electrode configurations are plotted in Fig. 5. The attenuation of the potentials due to distance along the radial axis was calculated and plotted in Fig. 6(A) and (B) for three electrode configurations bipolar, quasi-bipolar, and tri-polar. Fig. 6(A) shows the closed-form computer model attenuation plots for a single dipole signal, and Fig. 6(B) shows the attenuation plots for random dipole (noise added) simulations. From Fig. 6(A) and (B), the tri-polar electrode has greater

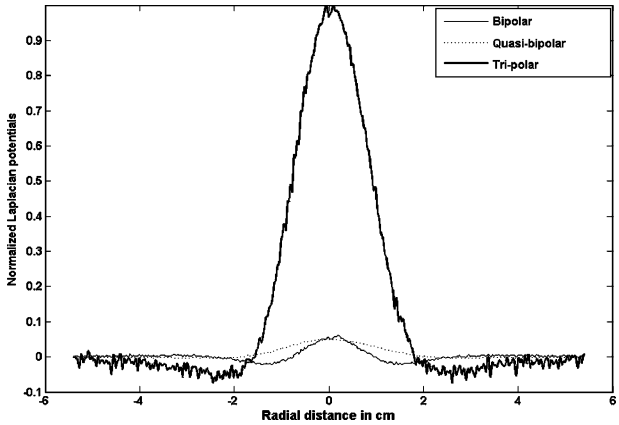

Fig. 5. Laplacian potentials measured from the tank experiments. The Laplacian potentials are normalized with maximum of tri-polar Laplacian potential.

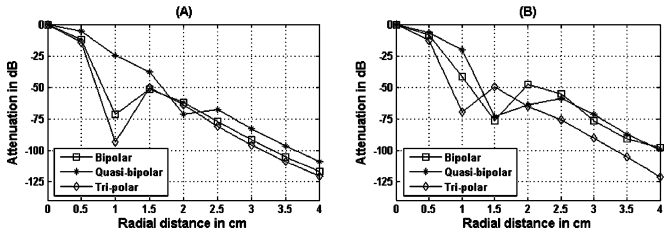

Fig. 6. Comparison of localization of three configurations. (A) Simulated attenuation from closed-form single moving dipole computer model. (B) Simulated attenuation from random dipole computer model.

attenuation with radial distance compared to bipolar and quasi-bipolar electrodes. A Bonferroni t test showed that there are statistically significant differences in the attenuation of off-center sources for bipolar, quasi-bipolar, and tri-polar concentric electrode configurations at the 1% significance level. The tri-polar electrode configuration had the steepest attenuation compared to the bipolar and quasi-bipolar electrode configurations.

C. Verification of Closed-Form Moving Dipole Computer Results With Tank Experimental Data

In Fig. 7, a comparison of attenuation in decibels was shown between the closed-form moving dipole computer model and measured tank experimental data for each of the three configurations, bipolar, quasi-bipolar, and tri-polar. Attenuation versus radial distance was plotted in each of the three panels with the tri-polar configuration having the greatest attenuation. A cross correlation was performed between the attenuation data of the closed-form moving dipole computer model and tank experiment data. The cross-correlation coefficient was 0.82 ± 0.1.

D. MRP Signals

The MRP signals recorded from subject 2 are representative of the signals acquired during the study from all subjects other than slight morphological differences and are shown in Fig. 8. Fig. 8(A) shows the signals recorded from gold disc electrodes. Fig. 8(B)–(D) shows the signals recorded from bipolar, quasi-bipolar and tri-polar 2.0-cm concentric ring electrodes, respectively. The quasi-bipolar signal is too small (0.125 μV peak-to-peak) to see at this scale and is shown with an inset. The

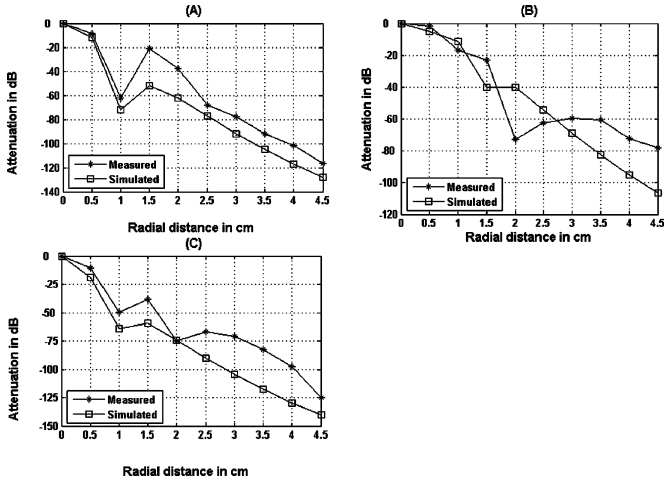

Fig. 7. Comparison of the simulated attenuation in decibels from the closed-form moving dipole computer model with the measured attenuation in decibels of Laplacian potentials from the tank experiments. (A) bipolar configuration, (B) quasi-bipolar configuration, and (C) tri-polar configuration.

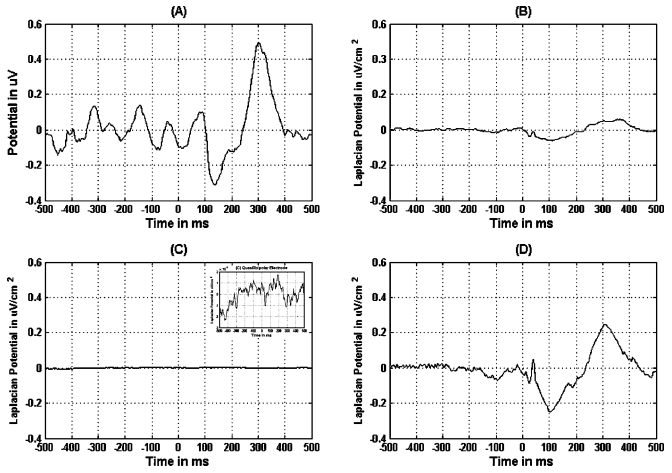

Fig. 8. The fast repetitive MRP signals recorded using (A) gold disc, (B) bipolar, (C) quasi-bipolar, and (D) tri-polar electrodes. The full-scale quasi-bipolar signal is shown with an inset.

tri-polar electrode recording exhibits sharp spikes and has the most localized MRP characteristics calculated by source separation [12]. In the recorded MRP signals two post movement peaks [16] are shown after the micro-switch was pressed. For the ten subjects tested, the average of the first post movement peak had a negative peak around 92 ms. The second postmovement peak had a positive peak around 275 ms. A Bonferroni t test showed that there are statistically significant differences in SNRs between gold disc, bipolar, quasi-bipolar, and tri-polar electrodes at the 1% significance level. For the MRP signals, the tri-polar electrode had the highest mean SNR of 30.46, followed by the bipolar, gold disc, and quasi-bipolar electrode with mean SNR of 20.22, 7.23, and 1.57, respectively.

V. Discussion

The results of the Bonferroni statistical analysis showed that there was a significant difference in approximating the Laplacian with the FPM, quasi-bipolar method, and NPM. The maximum error and relative error of the NPM are the least of the three methods. The maximum error and relative error of the tri-polar electrode configuration were less than those from the bipolar or quasi-bipolar electrode configurations. This is in accordance with what we expected. When estimating the surface Laplacian with the discrete methods, the NPM has more independent computed samples of the potentials than the other methods. The NPM has four more samples, which provides a closer approximation. For the closed-form model, the tri-polar electrode configuration calculates samples over the surface area with one more independent ring, which improves the estimate. Another characteristic in favor of the tri-polar electrode is that the approximation to the analytical Laplacian increases as the area sampled is decreased. The middle ring of the tri-polar electrode covers a smaller area, which helps improve the approximation.

From analysis of the measured tank experimental data and the simulated data for a 2-cm-diameter concentric ring electrode, it was determined that the tri-polar electrode had a greater localization capacity [20] than the bipolar and quasi-bipolar electrode configurations. This is confirmed by the results of Bonferroni t tests (at 1% significance level). As illustrated in Fig. 6(A) and (B), without/with noise sources, respectively, the tri-polar trace shows the greatest attenuation for off-center sources. This finding substantiates that the attenuation is greatest for the tri-polar electrode configuration when compared to bipolar and quasi-bipolar electrode configurations tested for global sources such as noise. It also demonstrates that the tri-polar electrode configuration is more sensitive to local signals as compared with the other configurations analyzed. This is illustrated by the width of the peaks. The tri-polar electrode peak is thinner than the others.

An evaluation of the attenuation traces in Fig. 7 suggests that the simplified computer model used is valid. The shapes of the attenuation of potentials for off-center sources comparing the three configurations in the computer modeled data are very similar (with correlation coefficient of 0.82 ± 0.1) to the measured data from the tank experiments. Since a unity dipole was used as the source of the computer model, it isn't possible to achieve a direct magnitude comparison between the computer model and the tank experiments. Use of a more realistic dipole source could help enhance these findings. Another area of our analysis that can be improved is to use multi-conductivity models, both for computer modeling and physical verification experiments. The different conductivities will alter the potentials calculated and measured, decreasing them if lower conductivities are used. Even with the reduced potentials, we should still achieve the same outcome that the tri-polar concentric ring electrode configuration was significantly better for accuracy and attenuation than the bipolar or quasi-bipolar concentric ring electrode configurations since the reduction of potentials should be relative to each configuration.

There are still other possible reasons for the difference between the simulated and measured values. This difference can be justified by a scaling factor, which originates from negligence in the computer model of conductivity for saltwater and permittivity of the printed circuit board material between the two thin

discs of copper used to construct the dipole. The tank experiments disclosed that there are also ambient noise sources and nonideal alignments of electrodes and dipoles that alter signals from the ideal conditions of the computer model, which is to be expected. More accurate computer models and higher precision mechanisms for positioning the dipoles and concentric ring electrodes in the tank experiments can help remedy these shortcomings.

The MRP signals for subject 2 are shown in Fig. 8. The MRP signals recorded with the tri-polar electrode configuration [Fig. 8(D)] shows the best localized activity and source separation with significantly better SNR than the bipolar, quasi-bipolar and gold disc electrodes. The significant improvement in SNR is promising and expected. This is due to the tri-polar concentric ring electrode attenuating off-center sources sharply such as artifacts originating from other areas of the body.

VI. Summary

The NPM is significantly better for approximating the analytical Laplacian than the FPM or the quasi-bipolar method. The tri-polar configuration results in significantly more accurate approximations to the analytical Laplacian than the bipolar and quasi-bipolar configurations. The tri-polar configuration is also significantly superior for attenuating global sources. There was a significant improvement in SNR using the tri-polar electrode to record MRP signals compared to bipolar, quasi-bipolar and the gold disc electrodes. These properties will be beneficial in localizing sources and rejecting global signals such as artifact from eye blinks. By detecting differences on the concentric electrode elements, it is possible to measure the potentials due to very localized brain activity with extremely high attenuation of global signals. With a dense array of these tri-polar concentric ring electrodes, it will be possible to record high spatial and temporal resolution LEEG. Further hardware development is necessary for the realization of an efficient LEEG mapping system utilizing the unique tri-polar concentric ring electrodes.

Acknowledgment

The authors thank all of the laboratory members, Dr. W. Jiang, Dr. C. Robinson, and Dr. A. Besio for their help with this research and manuscript.

References

[1] R. Srinivasan, "Methods to improve the spatial resolution of EEG," *J. Bioelectromagn.*, vol. 1, pp. 102–111, 1999.

[2] P. L. Nunez, R. B. Silberstein, P. J. Cadiush, J. Wijesinghe, A. F. Westdorp, and R. Srinivasan, "A theoretical and experimental study of high resolution EEG based on surface laplacians and cortical imaging," *EEG Clin. Neurophysiol.*, vol. 90, pp. 40–57, 1994.

[3] B. He, "Brain electrical source imaging: scalp laplacian mapping and cortical imaging," *Crit. Rev. Biomed. Eng.*, vol. 27, pp. 149–188, 1999.

[4] B. Hjorth, "An on-line transformation of EEG scalp potentials into orthogonal source derivations," *EEG. Clin. Neurophysiol.*, vol. 39, pp. 526–530, 1975.

[5] F. Perrin, O. Bertrand, and J. Pernier, "Scalp current density mapping: value and estimation from potential data," *IEEE Trans. Biomed. Eng.*, vol. BME-34, pp. 283–288, 1987.

[6] S. K. Law, P. L. Nunez, and R. S. Wijesinghe, "High resolution EEG using spline generated surface Laplacians on spherical and ellipsoidal surfaces," *IEEE Trans Biomed Eng*, vol. 40, no. 2, pp. 145–153, Feb. 1993.

[7] F. Babiloni, C. Babiloni, F. Carducci, L. Fattorini, P. Onorati, and A. Urbano, "Performances of surface laplacian estimators: a study of simulated and real scalp potential distributions," *Brain Topogr.*, vol. 8, pp. 35–45, 1995.

[8] ——, "Spline laplacian estimate of EEG potentials over a realistic magnet resonance constructed scalp surface model," *EEG Clin. Neurophysiol.*, vol. 98, pp. 363–373, 1996.

[9] B. He, J. Lian, and G. Li, "High-resolution EEG: a new realistic geometry spline laplacian estimation technique," *Clin. Neurophysiol.*, vol. 112, pp. 845–852, 2001.

[10] V. Fattorusso and J. Tilmant, "Exploration du champ electrique precordial a l'aide de deux electrodes circulaires, concentriques et rapprochees," *Arch. Mal du Coeur*, vol. 42, pp. 452–455, 1949.

[11] B. He and R. J. Cohen, "Body surface Laplacian ECG mapping," *IEEE Trans. Biomed. Eng.*, vol. 39, no. 11, pp. 1179–1191, Nov. 1992.

[12] D. Farino and C. Cescon, "Concentric-ring electrode systems for noninvasive detection of single motor unit activity," *IEEE Trans. Biomed. Eng.*, vol. 48, no. 11, pp. 1326–1334, Nov. 2001.

[13] W. Besio, K. Koka, and R. Patwardhan, "Computer simulation and tank experimental verification of concentric ring electrode," in *Proc. 26th Annu. Int. Conf. IEEE EMBC 2004*, 2004, vol. 3, pp. 2243–2246.

[14] W. Besio, R. Aakula, and W. Dai, "Comparison of bipolar vs tri-polar concentric ring laplacian estimates," in *Proc. 26th Annu. Int. Conf. IEEE EMBC 2004*, 2004, vol. 3, pp. 2255–2258.

[15] W. Besio, C. Lu, and P. Tarjan, "A feasibility study for body surface cardiac propagation maps of humans from laplacian moments of activation," *Electromagnetics*, vol. 21, pp. 621–632, 2001.

[16] B. Kopp, A. Kunkel, G. Muler, W. Muhlnickel, and H. Flor, "Steady-state movement related potentials evoked by fast repetitive moments," *Brain Topogr.*, vol. 13, pp. 21–28, 2000.

[17] G. Huiskamp, "Difference formulas for the surface laplacian on a triangulated surface," *J. Computational Phys.*, vol. 95, no. 2, pp. 477–496, 1991.

[18] L. Lapidus and G. F. Pinder, *Numerical Solution of Partial Differential Equations in Science and Engineering*. New York: Wiley, 1982, pp. 371–372.

[19] B. He and D. Wu, "Laplacian electrocardiography," *Crit. Rev. Biomed. Eng.*, vol. 27, no. 3–5, pp. 285–338, 1990.

[20] A. Van Oosterom and J. Strackee, "Computing the lead field of electrodes with axial symmetry," *Med. Biol. Eng. Comput.*, vol. 21, pp. 473–481, 1983.

[21] C. D. Klug, J. Silny, and G. Rau, "Improvement of spatial resolution in surface EMG: a theoretical and experimental comparison of different spatial filters," *IEEE Trans. Biomed. Eng.*, vol. 44, no. 7, pp. 567–574, Jul. 1997.

Walter G. Besio (S'92–M'02–SM'06) received the B.S.E.E. degree from University of Central Florida, Orlando, in 1993, and the M.S. and Ph.D. degrees in biomedical engineering from University of Miami, Coral Gables, FL, in 1997 and 2002, respectively.

From fall 2002 to present, he is an Assistant Professor in the Biomedical Engineering Department, Louisiana Tech University, Ruston. Prior to joining academia, he worked in the medical device and electronics industries for more than 12 years. His major research interests include electrode design, Laplacian EEG and ECG, biosignal detection and processing, neuro-stimulation, neuro-interfaces, and source localization.

Kanthaiah Koka received the B.E. degree in electronics and communication engineering from College of Engineering, Osmania University, Hyderabad, India, in 2002. He is working toward the Ph.D. degree in biomedical engineering at Louisiana Tech University, Ruston.

His current research involves Laplacian EEG, bioinstrumentation design, and biosignal processing.

Rajesh Aakula received the B. Tech degree in electrical and electronics from Jawaharlal Nehru Technical University, Hyderabad, India, in 2001. He received the M.S. degree in electrical engineering from Louisiana Tech University, Ruston, in 2004.

His research interests are Laplacian ECG and bioinstrumentation.

Weizhong Dai received the Ph.D. degree in applied mathematical and computational sciences from the University of Iowa, Iowa City, in 1994.

He is a McDermott International Professor of Mathematics at Louisiana Tech University, Ruston. His research interests include numerical solutions of partial differential equations, numerical heat transfer and bioheat transfer, numerical simulations for bioeffect of electromagnetics, and numerical methods for microfabrication systems, such as LCVD, melt crystallization, and X-ray lithography. He has published one book and more than 85 research articles in refereed journals and international conference proceedings.